SLAC-PUB-11046
BABAR-PROC-04/177
March 3, 2005

Beyond CP violation: hadronic physics at BaBar

Gabriella Sciolla
Massachusetts Institute of Technology, Department of Physics
Room 26-443, 77 Massachusetts Avenue, Cambridge, MA
(for the BaBar Collaboration)

Abstract

I report on recent studies of hadronic physics performed by the BaBar Collaboration. Emphasis is given to the measurement of the properties of newly discovered charmed hadrons and to the searches for light and heavy pentaquarks.

Contributed to the Proceedings of the First APS Topical Group Meeting on Hadron Physics
Fermilab, Batavia, IL (October 24-26, 2004).

Stanford Linear Accelerator Center, Stanford University, Stanford, CA 94309

Work supported by Department of Energy contracts DE-FC02-94ER40818 and
DE-AC02-76SF00515.

1 Introduction

The BaBar experiment [1] operates at the PEP-II e^+e^- asymmetric B-factory at SLAC. The abundant data sample of over $240\,\mathrm{fb}^{-1}$ to date, allows a rich and active research program. The primary goal of the experiment is to perform a quantitative test of the Standard Model, which can be achieved by precise measurements of CP violation in the B system, and of the CKM matrix elements related to the determination of the sides of the Unitarity Triangle. The study of B decays also provides a sensitive probe for New Physics beyond the Standard Model and allows for tests of Factorization, HQET, HQE and SCET.

In addition to studying B decays, BaBar is also active in the area of spectroscopy of lighter particles. This article focuses on two such topics: charm spectroscopy and searches for pentaquarks.

2 Recent results in charm spectroscopy

In 2003 BaBar discovered a narrow resonance [2] in the channel $D_s^+\pi^0$ with a mass of $2317\,\mathrm{MeV}/c^2$. The existence of this state, named $D_{sJ}^*(2317)^+$, was soon confirmed by CLEO [3] and Belle [4]. Subsequently, the CLEO Collaboration discovered another $D_s^{*+}\pi^0$ narrow state [3], the $D_{sJ}(2460)^+$, promptly confirmed by BaBar [4] and Belle [5].

The discovery of the D_{sJ} resonances received a lot of attention by the theoretical community and revived the entire field of charm spectroscopy. Many hypotheses were formulated to explain the unexpected narrow widths and masses of these states that are not in agreement with the theoretical predictions. These resonances are usually interpreted as P-wave $c\overline{s}$ quark states [6–9], although other interpretations [10–14] cannot be ruled out.

In this section I will report on the improved measurements of the properties of the $D_{sJ}^*(2317)^+$ and $D_{sJ}(2460)^+$ [15, 16]. I will also review the recently published evidence for the $X(3872)$ [17] and the status of the search for the $D_{sJ}(2632)^+$ [18].

2.1 Mass of the $D_{sJ}^*(2317)^+$ and $D_{sJ}(2460)^+$ in $e^+e^- \to c\overline{c}$

BaBar recently published [16] new measurements for the masses of the $D_{sJ}^*(2317)^+$ and $D_{sJ}(2460)^+$. This analysis, based on a dataset of 125 fb^{-1}, reconstructs the D_{sJ} resonances produced in $c\overline{c}$ events in four final states: $D_s^+\pi^0$, $D_s^+\gamma$, $D_s^+\pi^0\gamma$, and $D_s^+\pi^+\pi^-$. The D_s^+ candidates are reconstructed in $K^+K^-\pi^+$ through $\overline{K}^{*0}K^+$ and $\phi\pi^+$ intermediate states. The D_{sJ} candidates are obtained by forming invariant mass combinations of the reconstructed D_s^+ mesons with π^0, γ, and $\pi^\pm$ particles.

Figure 1 (left) shows the invariant mass of the $D_{sJ}^*(2317)^+$ candidates reconstructed in the $D_s^+\pi^0$ final state. A clear $D_{sJ}^*(2317)^+$ signal is visible on top of the combinatorial background. Reflections from $D_{sJ}(2460)^+ \to D_s^+\pi^0\gamma$ and $D_s^*(2112)^+ \to D_s^+\gamma$ are shown in dark and light gray, respectively. A likelihood fit measures a signal yield of 1275 ± 45 and an invariant mass of

$$m(D_{sJ}^*(2317)^+) = (2318.9 \pm 0.3\ (\mathrm{stat.}) \pm 0.9\ (\mathrm{syst.}))\,\mathrm{MeV}/c^2.$$

Figure 1 (right) shows the $D_{sJ}(2460)^+$ invariant mass in the $D_s^+\gamma$ final state. The signal is clearly visible on top of a falling combinatorial background. The broader peak centered around $2.3\,\mathrm{GeV}/c^2$ is a combination of two reflections. The larger reflection is due to D_s^+ mesons from the decay $D_{sJ}^*(2317)^+ \to D_s^+\pi^0$ combined with one of the photons from the π^0; the other is produced in a similar fashion from $D_{sJ}(2460)^+ \to D_s^+\pi^0\gamma$ decay. A signal of 509 ± 46 $D_{sJ}(2460)^+$ candidates

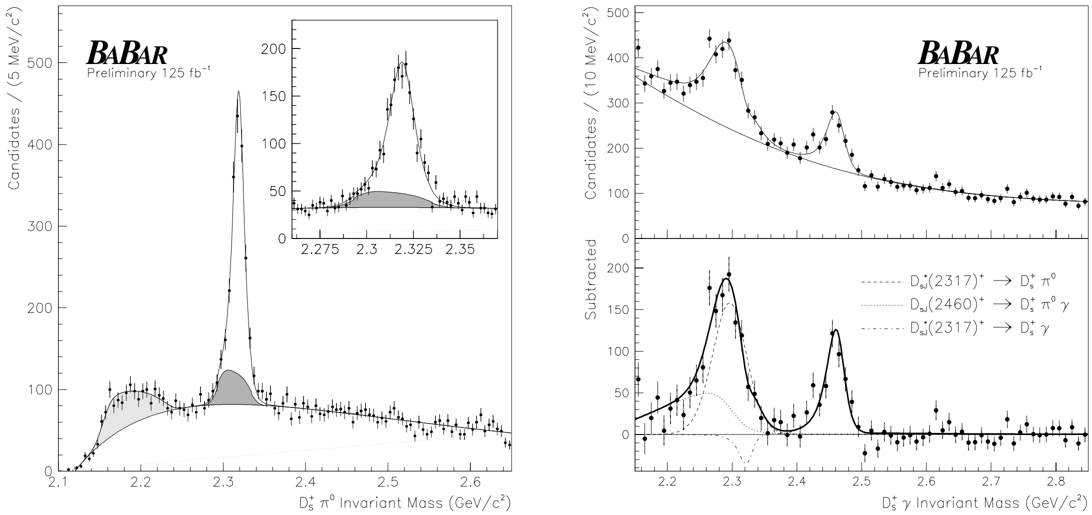

Figure 1: Left: $D_s^+\pi^0$ invariant mass distribution. The solid curve is the result of an unbinned likelihood fit. The dark (light) gray region is the contribution from the $D_{sJ}(2460)^+ \to D_s^+\pi^0\gamma$ ($D_s^*(2112)^+ \to D_s^+\gamma$) reflection. The inset is an expanded view near the $D_{sJ}^*(2317)^+$ mass. Right: $D_s^+\gamma$ invariant mass distribution before (top) and after (bottom) subtraction of the combinatorial background. The solid curve is the result of an unbinned likelihood fit. Various contributions to the signal and reflection portions of the fit are overlaid (dashed lines).

allows us to measure

$$m(D_{sJ}(2460)^+ \to D_s^+\gamma) = (2457.2 \pm 1.6\ (\text{stat.}) \pm 1.3\ (\text{syst.}))\,\text{MeV}/c^2.$$

Figure 2 (left) illustrates the invariant mass distribution for the $D_{sJ}(2460)^+$ decaying into $D_s^+\pi^0\gamma$. This three body decay is dominated by the intermediate state $D_s^*(2112)^+\pi^0$. A likelihood fit yields a signal of 292 ± 29 $D_{sJ}(2460)^+$ events. Two reflections are visible in the distribution: the light gray shoulder is due to $D_s^*(2112)^+ \to D_s^+\gamma$ decays; the dark gray peaking background is due to $D_{sJ}^*(2317)^+ \to D_s^+\pi^0$ decays combined with unassociated photons. The position and shape of the reflections is extracted from Monte Carlo simulation and validated on the data side bands as shown in figure 2 left-top and left-bottom plots. The mass of the $D_{sJ}(2460)^+$ extracted from this measurement is

$$m(D_{sJ}(2460)^+ \to D_s^+\pi^0\gamma) = (2459.1 \pm 1.3\ (\text{stat.}) \pm 1.2\ (\text{syst.}))\,\text{MeV}/c^2.$$

Figure 2 (right) shows the invariant mass of the $D_{sJ}(2460)^+$ candidates reconstructed in the $D_s^+\pi^+\pi^-$ final state. A signal of 67 ± 11 $D_{sJ}(2460)^+$ decays is clearly visible on top of the combinatorial background; a second peak due to 124 ± 18 $D_{s1}(2536)^+$ particles is also evident. The masses for these two particles are extracted by using a likelihood fit:

$$\begin{aligned} m(D_{sJ}(2460)^+ \to D_s^+\pi^+\pi^-) &= (2460.1 \pm 0.3\ (\text{stat.}) \pm 1.2\ (\text{syst.}))\,\text{MeV}/c^2, \\ m(D_{s1}(2536)^+) &= (2534.3 \pm 0.4\ (\text{stat.}) \pm 1.2\ (\text{syst.}))\,\text{MeV}/c^2. \end{aligned}$$

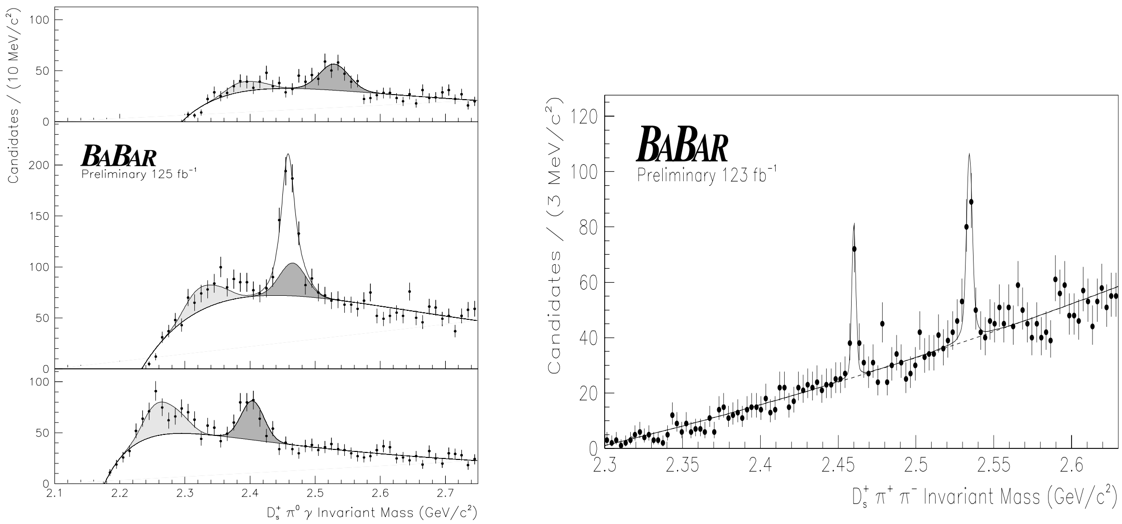

Figure 2: Left: $D_s^+\pi^0\gamma$ mass spectrum of the events that fall in the $D_s^+\gamma$ signal region (center plot), the $D_s^+\gamma$ high mass sideband (top plot), and the low mass sideband (bottom plot). Reflections from (dark gray) $D_{sJ}^*(2317)^+ \to D_s^+\pi^0$ and (light gray) $D_s^*(2112)^+ \to D_s^+\gamma$ decays appear well modeled in the Monte Carlo. Right: $D_s^+\pi^+\pi^-$ invariant mass distribution for candidates that satisfy the requirements discussed in the text. The solid curve is the result of an unbinned likelihood fit.

The mass measurements mentioned above are combined to obtain the following average:

$$m(D_{sJ}(2460)^+) \quad = \quad (2459.4 \pm 0.3 \text{ (stat.)} \pm 1.0 \text{ (syst.)})\,\mathrm{MeV}/c^2.$$

By combining the efficiency corrected yields, the following relative branching fractions are measured:

$$\frac{\mathcal{B}(D_{sJ}(2460)^+ \to D_s^+\gamma)}{\mathcal{B}(D_{sJ}(2460)^+ \to D_s^+\pi^0\gamma)} = 0.375 \pm 0.054 \text{ (stat.)} \pm 0.057 \text{ (syst.)},$$

$$\frac{\mathcal{B}(D_{sJ}(2460)^+ \to D_s^+\pi^+\pi^-)}{\mathcal{B}(D_{sJ}(2460)^+ \to D_s^+\pi^0\gamma)} = 0.082 \pm 0.018 \text{ (stat.)} \pm 0.011 \text{ (syst.)}.$$

2.2 Properties of $D_{sJ}^*(2317)^+$ and $D_{sJ}(2460)^+$ from exclusive B decays

Pure samples of $D_{sJ}^*(2317)^+$ and $D_{sJ}(2460)^+$ can be obtained by exclusive reconstruction of the decay $B \to D_{sJ}^{(*)+}\overline{D}^{(*)}$ [15]. This analysis, performed on a sample of $113\,\mathrm{fb}^{-1}$, measures the spin and branching fractions of the D_{sJ} resonances.

The $\overline{D}$ and D_s^+ mesons are reconstructed in the following decay modes: $\overline{D}^0 \to K^+\pi^-$, $K^+\pi^-\pi^0$, $K^+\pi^-\pi^+\pi^-$; $D^- \to K^+\pi^-\pi^-$; $D_s^+ \to \phi\pi^+$ ($\phi \to K^+K^-$), $\overline{K}^{*0}K^+$ ($\overline{K}^{*0} \to K^-\pi^+$). The D^* candidates are reconstructed in the decay modes $D^{*+} \to D^0\pi^+$, $D^{*0} \to D^0\pi^0$, $D^0\gamma$, and $D_s^* \to D_s^+\gamma$. The selected pairs of $D_s^{(*)+}$ and $\overline{D}^{(*)}$ candidates are combined with a photon or a π^0 to complete the B decay. Cuts on the energy and invariant mass of the B candidate are used to enhance the purity of the signal.

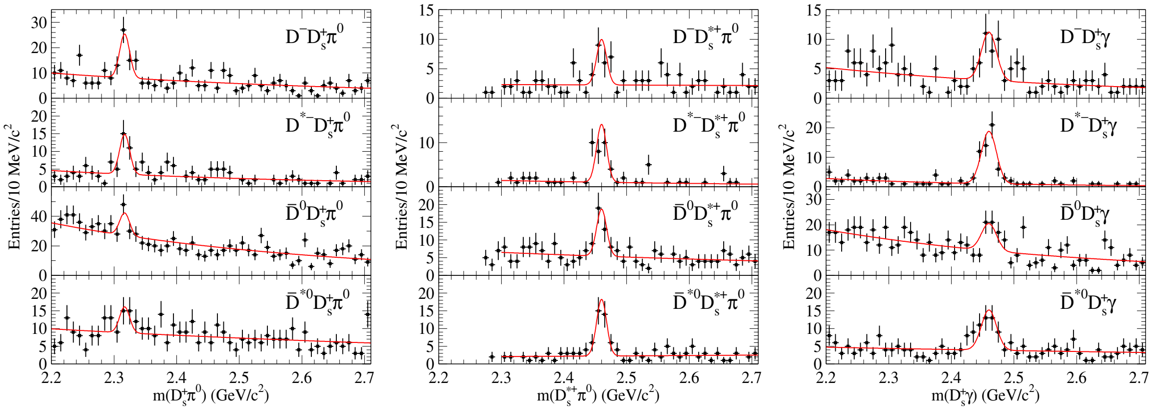

Figure 3: $D_s^+\pi^0$ (left), $D_s^{*+}\pi^0$ (center), and $D_s^+\gamma$ (right) mass spectra of the selected B signal candidates for the 12 $\overline{D}^{(*)}D_{sJ}$ final states. Curves are the results of the fits.

Figure 3 shows the D_{sJ} invariant mass for the selected B candidates for 12 different $\overline{D}^{(*)}D_{sJ}$ final states. The yields, the corresponding branching fractions and the statistical significance of each channel are listed in Table 1.

From the measured branching fractions for $B \to D_{sJ}^+(2460)\overline{D}^{(*)}$ in $D_s^{*+}\pi^0$ and in $D_s^+\gamma$, we find the ratio

$$\frac{\mathcal{B}(D_{sJ}(2460)^+ \to D_s^+\gamma)}{\mathcal{B}(D_{sJ}(2460)^+ \to D_s^{*+}\pi^0)} = 0.274 \pm 0.045 \pm 0.020,$$

in agreement with the prediction from [7].

A helicity analysis is performed for the $D_{sJ}(2460)^+$ state, using the decays $B^+ \to D_{sJ}(2460)^+\overline{D}^0$ and $B^0 \to D_{sJ}(2460)^+D^-$, with $D_{sJ}(2460)^+ \to D_s^+\gamma$. The helicity angle θ_h is defined as the angle between the D_{sJ} momentum in the B-meson rest frame and the D_s momentum in the D_{sJ} rest frame. Figure 4 shows the resulting angular distribution, corrected for detector acceptance and selection efficiency. The data exclude the $J = 2$ hypothesis (χ^2/n.d.f.=36.4/4), while they are in good agreement with the hypothesis of $J = 1$ (χ^2/n.d.f.=4.0/4). A $J = 0$ spin is ruled out by parity and angular momentum conservation in the decay $D_{sJ}(2460)^+ \to D_s^+\gamma$.

2.3 Observation of the $X(3872)$ in B decays

A new state, known as $X(3872)$, was recently discovered by the Belle Collaboration [19] and confirmed by CDF [20]. This state, reconstructed in the final state $J/\psi\pi^+\pi^-$, is probably a charmonium candidate for the state 1^3D_2 ($J^{PC} = 2^{--}$) or 1^3D_3 ($J^{PC} = 3^{--}$) [21], but could also be a molecule of D and D^* mesons [22].

BaBar recently confirmed the existence of this particle [17]. The analysis, based on 117 million $B\overline{B}$ events, reconstructs the $X(3872)$ in the final state $J/\psi\pi^+\pi^-$ for $X(3872)$ produced in the decay $B^- \to X(3872)K^-$. A total of 30.6 ± 5.8 events are reconstructed. The mass of the $X(3872)$ is measured to be $m(X(3872)) = (3873.4 \pm 1.4)\,\mathrm{MeV}/c^2$, and the product branching fraction $\mathcal{B}(B^- \to X(3872)K^-) \times \mathcal{B}(X(3872) \to J/\psi\pi^+\pi^-) = (1.28 \pm 0.41) \times 10^{-5}$ is obtained.

Table 1: Event yields, final branching fractions $\mathcal{B}$, and significance for $B \to D_{sJ}^{(*)+}\overline{D}^{(*)}$ decays. The first error on $\mathcal{B}$ is statistical, the second is systematic, and the third is from the $\overline{D}$ and D_s^+ branching fractions.

B mode		Yield	$\mathcal{B}(10^{-3})$	Significance
$B^0 \to D_{sJ}^*(2317)^+ D^-$	$[D_s^+\pi^0]$	34.7 ± 8.0	$1.8 \pm 0.4 \pm 0.3^{+0.6}_{-0.4}$	5.5
$B^0 \to D_{sJ}^*(2317)^+ D^{*-}$	$[D_s^+\pi^0]$	23.5 ± 6.1	$1.5 \pm 0.4 \pm 0.2^{+0.5}_{-0.3}$	5.2
$B^+ \to D_{sJ}^*(2317)^+ \overline{D}^0$	$[D_s^+\pi^0]$	32.7 ± 10.8	$1.0 \pm 0.3 \pm 0.1^{+0.4}_{-0.2}$	3.1
$B^+ \to D_{sJ}^*(2317)^+ \overline{D}^{*0}$	$[D_s^+\pi^0]$	17.6 ± 6.8	$0.9 \pm 0.6 \pm 0.2^{+0.3}_{-0.2}$	2.5
$B^0 \to D_{sJ}(2460)^+ D^-$	$[D_s^{*+}\pi^0]$	17.4 ± 5.1	$2.8 \pm 0.8 \pm 0.5^{+1.0}_{-0.6}$	4.2
$B^0 \to D_{sJ}(2460)^+ D^{*-}$	$[D_s^{*+}\pi^0]$	26.5 ± 5.7	$5.5 \pm 1.2 \pm 1.0^{+1.9}_{-1.2}$	7.4
$B^+ \to D_{sJ}(2460)^+ \overline{D}^0$	$[D_s^{*+}\pi^0]$	29.0 ± 6.8	$2.7 \pm 0.7 \pm 0.5^{+0.9}_{-0.6}$	5.1
$B^+ \to D_{sJ}(2460)^+ \overline{D}^{*0}$	$[D_s^{*+}\pi^0]$	30.5 ± 6.4	$7.6 \pm 1.7 \pm 1.8^{+2.6}_{-1.6}$	7.7
$B^0 \to D_{sJ}(2460)^+ D^-$	$[D_s^+\gamma]$	24.8 ± 6.5	$0.8 \pm 0.2 \pm 0.1^{+0.3}_{-0.2}$	5.0
$B^0 \to D_{sJ}(2460)^+ D^{*-}$	$[D_s^+\gamma]$	53.0 ± 7.8	$2.3 \pm 0.3 \pm 0.3^{+0.8}_{-0.5}$	11.7
$B^+ \to D_{sJ}(2460)^+ \overline{D}^0$	$[D_s^+\gamma]$	31.9 ± 9.0	$0.6 \pm 0.2 \pm 0.1^{+0.2}_{-0.1}$	4.3
$B^+ \to D_{sJ}(2460)^+ \overline{D}^{*0}$	$[D_s^+\gamma]$	34.6 ± 7.6	$1.4 \pm 0.4 \pm 0.3^{+0.5}_{-0.3}$	6.0

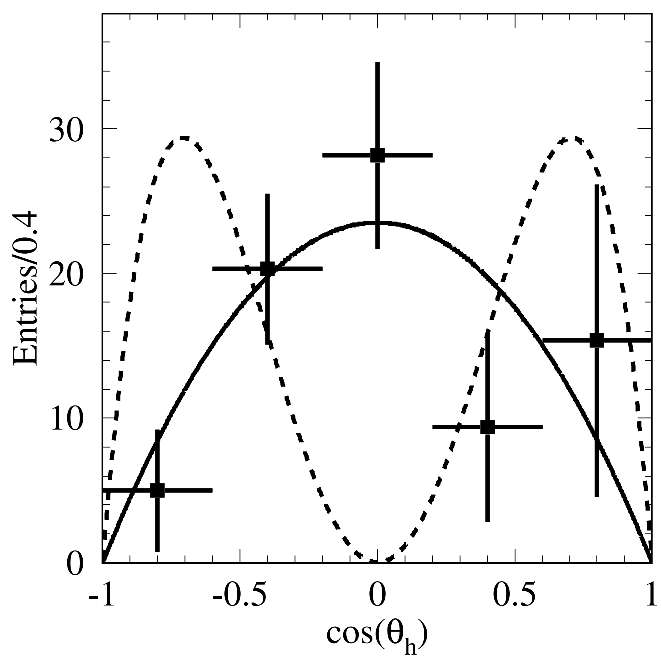

Figure 4: Helicity distribution obtained from $m(D_s\gamma)$ fits in bins of $\cos(\theta_h)$ for data (points) in comparison with the expectations for a $D_{sJ}(2460)^+$ spin $J = 1$ (solid line) and $J = 2$ (dashed line), respectively, after normalizing the predicted spectra to the data.

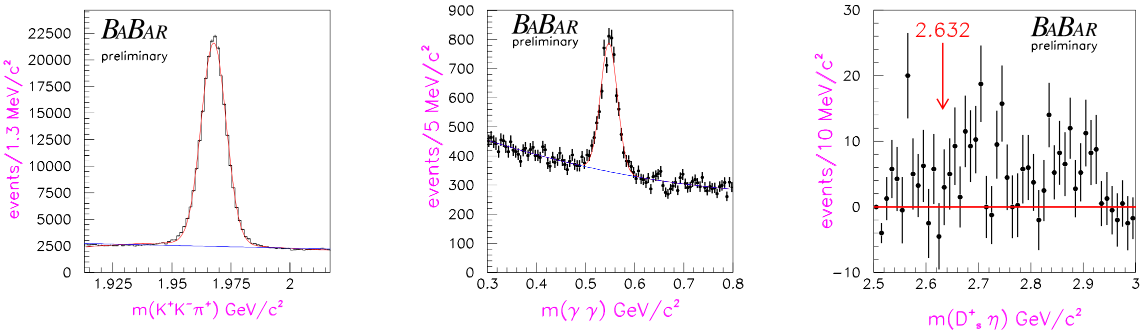

Figure 5: $K^+K^-\pi^+$ (left), $\gamma\gamma$ (middle), and $D_s^+\eta$ (right) invariant mass distributions in $125\,\mathrm{fb}^{-1}$.

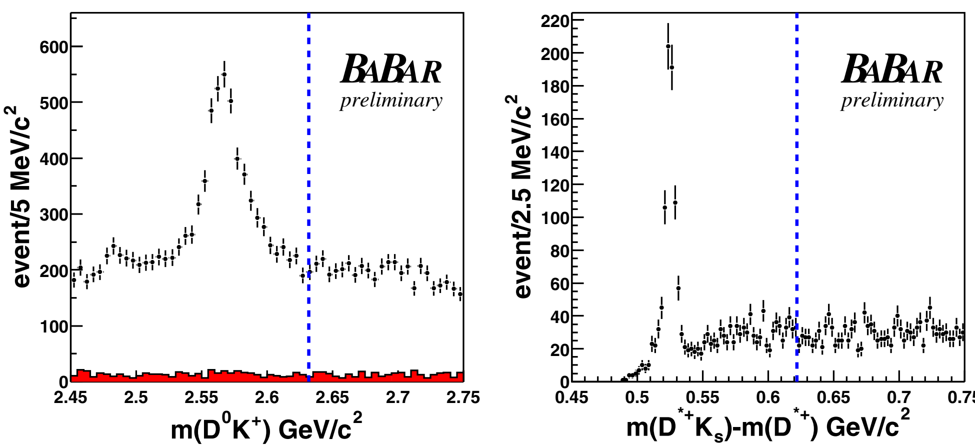

Figure 6: D^0K^+ (left) and $D^{*+}K_S^0$ (right) invariant mass distributions in $125\,\mathrm{fb}^{-1}$.

2.4 Search for the $D_{sJ}^*(2632)^+$ meson

A narrow state decaying to $D_s^+\eta$, named $D_{sJ}^*(2632)^+$, has been recently observed by the SELEX Collaboration [23]. BABAR has searched for this resonance in the final states $D_s^+\eta$, D^0K^+ and $D^{*+}K_S^0$. The analysis, based on $125\,\mathrm{fb}^{-1}$, aims to reconstruct D_{sJ} states produced in $e^+e^- \to c\overline{c}$ events.

Figure 5 shows the abundant and clean samples of $D_s^+ \to K^+K^-\pi^+$ (left) and $\eta \to \gamma\gamma$ (middle) used for this analysis. The background subtracted invariant mass of the $D_s^+\eta$ system is shown in figure 5 (right). No signal is evident in the region around $2632\,\mathrm{MeV}/c^2$. Figure 6 shows the invariant mass of the systems D^0K^+ (left) and $D^{*+}K_S^0$ (right). These distributions show very clear signals for the decays $D_{s2}(2573)^+ \to D^0K^+$ and $D_{s1}(2536)^+ \to D^{*+}K_S^0$, but no accumulation where the $D_{sJ}^*(2632)$ is expected.

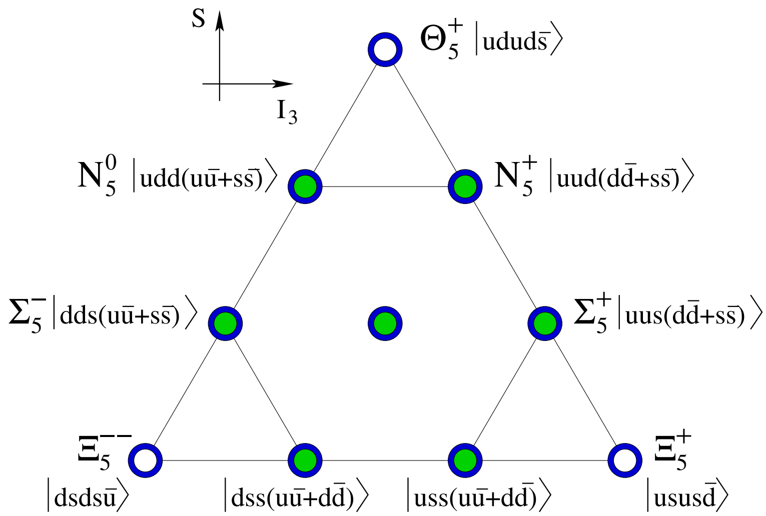

Figure 7: Light pentaquark anti-decuplet and octet.

3 Pentaquark searches at BABAR

In the past two years, several experiments reported evidence for new baryon states that are compatible with being bound states of five quarks (pentaquarks). The most convincing evidence is for an exotic ($B = 1$, $S = 1$), light resonance called $\Theta^+(1540)$ [24–30]. This state has an unusually narrow width for a particle that could decay strongly. Recently, NA49 published evidence for two heavier narrow states (Ξ^{--} and Ξ^0) [31], while H1 observed a narrow exotic charmed resonance (Θ_c^0) with mass of $3099\,\mathrm{MeV}/c^2$ [32].

Several theoretical models have been proposed to describe the pentaquark structure [33–35]. The prediction is that the lowest mass states containing u, d and s quarks should occupy a spin-$\frac{1}{2}$ anti-decuplet and octet as illustrated in figure 7.

Although experiments with baryon beams may have an advantage in producing these states, we know that e^+e^- collisions produce quite democratically all of the other particles. It has been experimentally observed that for baryons with non-zero B, C or strangeness, and/or orbital angular momentum, the production rates seem to depend only on mass and spin, and not on the quark content. If pentaquarks are produced similarly, their production rate should be as high as that for ordinary baryons of the same mass and spin, i.e., about 8×10^{-4} for the $\Theta_5^+(1540)$ and 4×10^{-5} for the Θ_5^{--} [36].

It has been recently suggested that heavier pentaquarks such as the Θ^{*++} could be accessible at the B factories. The Θ^{*++} is a member of the baryon 27-plet containing the quarks $uuud\overline{s}$ and has $I = 1$ and $I_3 = 1$. It is predicted to decay into the final state pK^+, and to have a mass between 1.43 and $1.70\,\mathrm{GeV}/c^2$ with a width of 37–80 MeV/c^2 [37].

In this section I discuss the results of several searches for light [38] and heavy [39] pentaquarks recently published by BaBar. Light strange pentaquarks belonging to the decuplet and octet represented in figure 7 are inclusively searched for in $123\,\mathrm{fb}^{-1}$. The analysis focuses on final states containing strange particles and protons that are easily identifiable in the detector. The search for the Θ^{*++} follows a very different approach, involving the exclusive reconstruction of B^+ mesons decaying into $p\overline{p}K$ final states, as suggested in [40]. This analysis is performed with $81\,\mathrm{fb}^{-1}$.

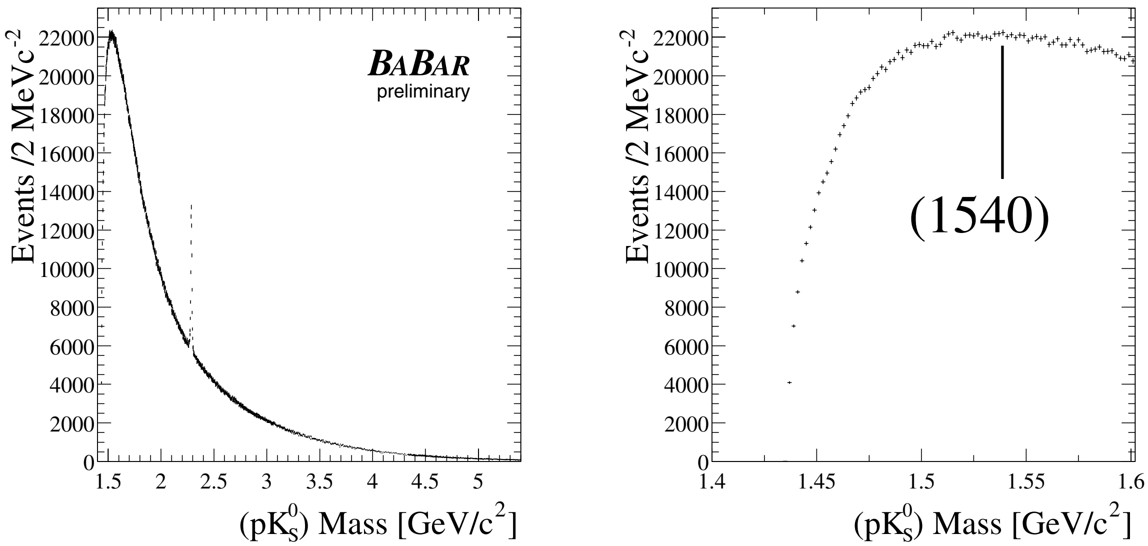

Figure 8: pK^0_S invariant mass distributions in the $\Theta^+_5(1540)$ search.

3.1 Search for $\Theta^+_5(1540) \to pK^0_S$

This analysis aims to reconstruct decays of the $\Theta^+_5(1540)$ into the pK^0_S final state. The K^0_S candidates are reconstructed in their decay into two charged pions, with selection criteria designed to avoid a bias toward any specific production mechanism, while keeping a high reconstruction efficiency. The K^0_S candidates are then combined with protons from the interaction point to form the $\Theta^+_5(1540)$ candidates.

The invariant mass distribution of the pK^0_S pairs is shown in figure 8. The clear peak around $2285\,\mathrm{MeV}/c^2$ visible on the left plot is due to the decay $\Lambda^+_c \to pK^0_S$. The abundant signal and the narrow peak demonstrate our sensitivity to the presence of a narrow resonance. The left plot of figure 8 is a magnified view of the region where the $\Theta^+_5(1540)$ is expected. No signal is observed. Null results are obtained also when the search is performed separately for ten momentum bins uniformly distributed between zero and $5\,\mathrm{GeV}/c$.

The null results are used to set a limit on the differential production cross section of $\Theta^+_5(1540)$ in e^+e^- interaction. In the calculation the mass is assumed to be $1540\,\mathrm{MeV}/c^2$. Since the natural width of this particle is unknown, two hypotheses have been considered: $\Gamma = 8\,\mathrm{MeV}/c^2$, corresponding to the experimental upper limit, and $\Gamma = 1\,\mathrm{MeV}/c^2$, corresponding to a very narrow state. The 95% C.L. upper limit on the differential production cross section of the $\Theta^+_5(1540)$ is shown in figure 9. The branching fraction $\mathcal{B}(\Theta^+_5(1540) \to pK^0_S)$ is assumed to be 1/4. Taking the upper limit width, the 95% C.L. upper limit on the total production rate is calculated to be 1.1×10^{-4} per $q\overline{q}$ event, roughly a factor of eight below the values measured for ordinary baryons of similar mass as shown in figure 10.

3.2 Search for $\Xi^{--}_5 \to \Xi^-\pi^-$ and $\Xi^0_5 \to \Xi^-\pi^+$

The Ξ^{--}_5 and Ξ^0_5 states were searched for in decays involving Ξ^- baryon and a charged pion. The Ξ^- is reconstructed in its decay $\Xi^- \to \Lambda^0\pi^-$ with $\Lambda^0 \to p\pi^-$. As for the $\Theta^+_5(1540)$ search, all

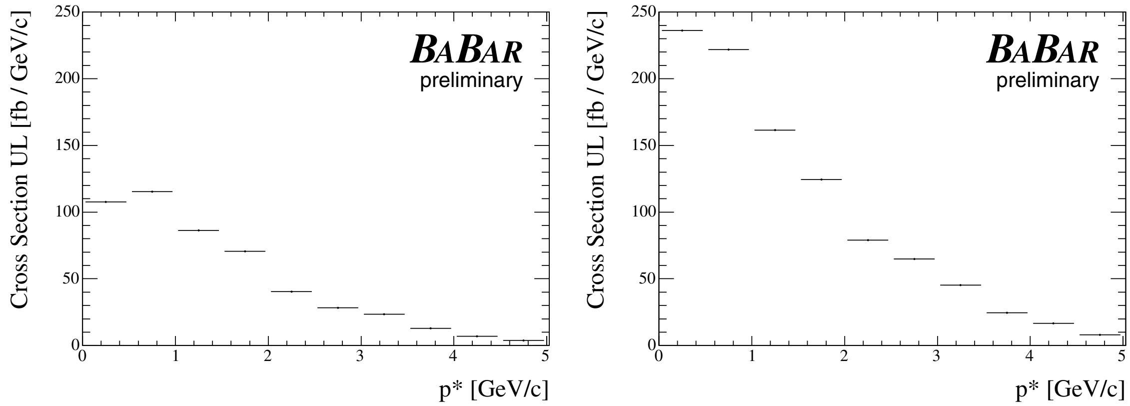

Figure 9: 95% C.L. upper limit of the differential production cross section of $e^+e^- \to \Theta_5^+(1540)X$, assuming $\Gamma = 8\,\mathrm{MeV}/c^2$ (left) and $1\,\mathrm{MeV}/c^2$ (right).

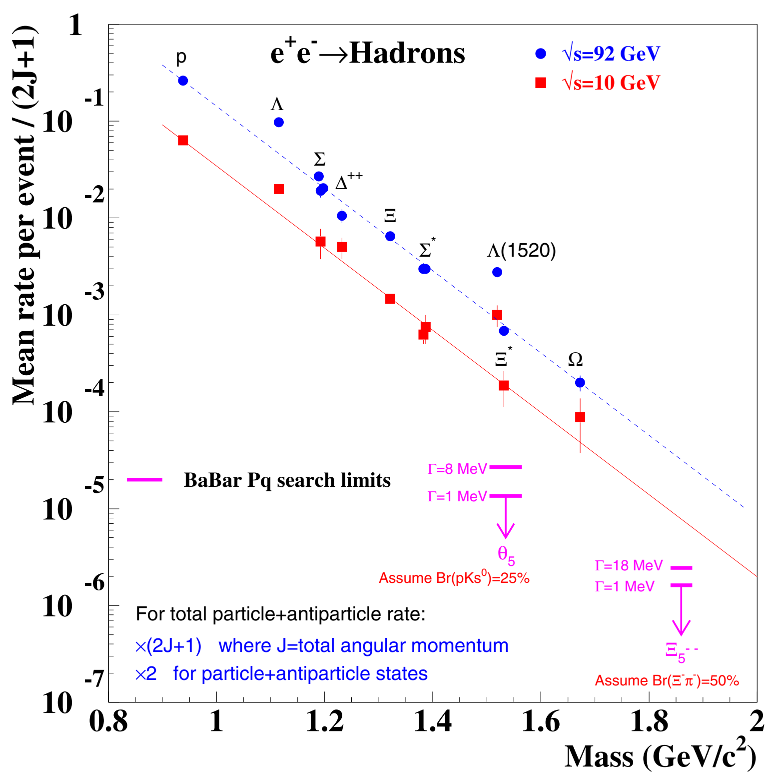

Figure 10: Baryon production rates in e^+e^- interactions [36] measured at the Z^0 pole (circles) and $\Upsilon(4S)$ (squares). The vertical axis accounts for number of spin and particle+antiparticle states. The lines are chosen to guide the eye. The arrows indicate the upper limits on the Θ_5^+ and Ξ_5^{--}.

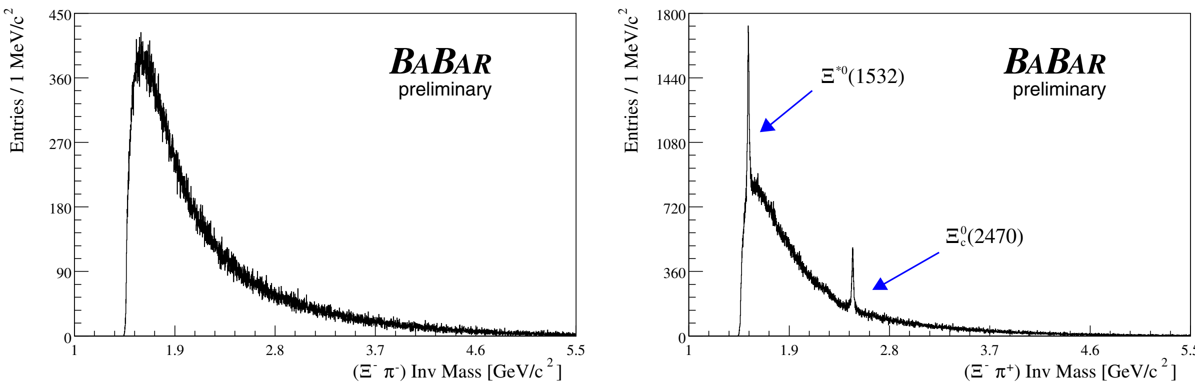

Figure 11: $\Xi^-\pi^-$ (left) and $\Xi^-\pi^+$ (right) invariant mass distributions in the Ξ_5^{--} and Ξ_5^0 searches.

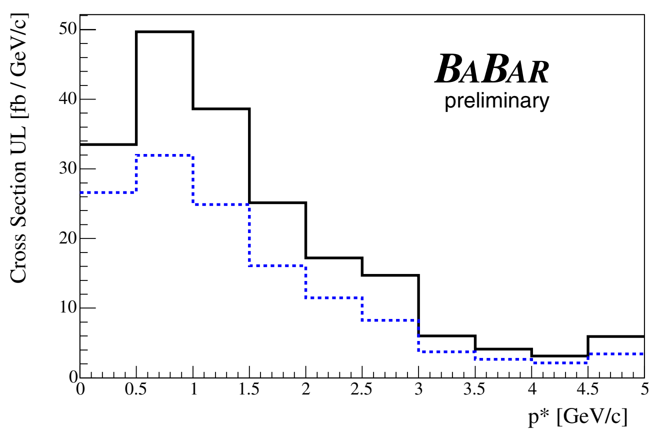

Figure 12: 95% C.L. upper limit of the differential production cross section of $e^+e^- \to \Xi_5^{--}X$, assuming $\Gamma = 18\,\mathrm{MeV}/c^2$ (solid line) and $1\,\mathrm{MeV}/c^2$ (dotted line).

selection criteria used in the analysis are designed to maximize the efficiency and avoid a bias toward any specific production mechanism.

The invariant mass distributions for the $\Xi^-\pi^-$ and $\Xi^-\pi^+$ pairs are illustrated in figure 11. No resonance is visible in the $\Xi^-\pi^-$ invariant mass distribution. Two peaks are instead visible in the $\Xi^-\pi^+$ plot, corresponding to the decays of $\Xi^{*0}(1532)$ and $\Xi_c^0(2470)$, but no structure is visible in the region where the Ξ_5^0 is expected.

The absence of a Ξ_5^{--} signal is reflected as an upper limit at the 95% C.L. on the differential production cross section shown in figure 12 as a function of p^*, the momentum in the e^+e^- center of mass frame. The branching fraction $\mathcal{B}(\Xi_5^{--} \to \Xi^-\pi^-)$ is assumed to be 1/2. Assuming a width of $18\,\mathrm{MeV}/c^2$, the 95% C.L. upper limit on the total production rate is calculated to be 1.0×10^{-5} per $q\overline{q}$ event, roughly a factor of two below the values measured for ordinary baryon of similar mass as illustrated in figure 10.

3.3 Inclusive searches for other strange pentaquarks

BaBar also performs a more inclusive search for other strange pentaquarks decaying into the final states $\Lambda^0 K$ and $\Sigma^0 K$, where K is either a charged or a neutral kaon and $\Sigma^0 \to \Lambda^0\gamma$ and $\Lambda^0 \to p\pi^-$. These final states give access to the pentaquarks Ξ_5^-, Ξ_5^0, N_5^0 and N_5^+ introduced in figure 7. Inclusive searches are also performed for $\Sigma_5^+ \to pK_S^0$. No pentaquark signal is observed in any of these inclusive searches.

3.4 Search for the Θ^{*++} pentaquark in exclusive B decays

In this analysis, the B^+ mesons are exclusively reconstructed in the $p\overline{p}K^+$ final state. The purity of the signal is increased by cuts on the invariant mass and energy of the B candidate, and by the use of topological variables that distinguish continuum from $B\overline{B}$ events. Of the 212 candidates reconstructed in this analysis, 188 ± 17 are estimated to be real B^+ decays, including 68 ± 10 containing charmonium decays to $p\overline{p}$.

The pK^+ invariant mass distribution of the selected B candidates is analyzed searching for a pentaquark signal up to $2.36\,\mathrm{GeV}/c^2$. No events are observed below $1.85\,\mathrm{GeV}/c^2$, and no structure is visible in the entire area studied. The 95% C.L. upper limit for the branching fraction of $B^+ \to \Theta^{*++}(pK^+)\overline{p}$ is measured to be 1.5×10^{-7} for $1.43 < m(\Theta^{*++}) < 1.85\,\mathrm{GeV}/c^2$, 2.4×10^{-7} for $1.85 < m(\Theta^{*++}) < 2.00\,\mathrm{GeV}/c^2$, and 3.3×10^{-7} for $2.00 < m(\Theta^{*++}) < 2.36\,\mathrm{GeV}/c^2$.

4 Summary

Many new results in the field of hadronic physics were recently published by the BaBar Collaboration.

The discovery of the $D_{sJ}^*(2317)^+$ narrow state revived the interest in charm spectroscopy. The mass of the $D_{sJ}^*(2317)^+$ and of its heavier twin, the $D_{sJ}(2460)^+$, are now measured with high precision in many different decay modes. In addition, the measurement of other properties, such as branching fractions and angular distributions, are now accessible, thanks to the pure samples of D_{sJ} mesons reconstructed in B decays.

The narrow state $X(3872)$ has recently been observed by BaBar, in agreement with previous results from Belle. The $D_{sJ}(2632)$ state reported by SELEX, on the other hand, has not been confirmed.

BaBar also searches for pentaquark production in e^+e^- interactions. Various states are investigated, and particular attention is given to the searches for the $\Theta_5^+(1540)$ and the $\Xi^{--}(1860)$. The null results reflect limits on the rates of the production of such states in e^+e^- events, well below the rates measured for ordinary baryons of similar masses.

Acknowledgments

It is a pleasure to thank my BaBar colleagues P. Burchat, V. Halyo, V. Luth, M. Morii and R. Yamamoto for helpful comments. I would also like to thank the organizers of the APS Topical Group on Hadronic Physics for creating such a pleasant and productive environment. This work was supported by the DOE contracts DE-FC02-94ER40818 and DE-AC02-76SF00515.

References

[1] B. Aubert *et al.* [BABAR Collaboration], Nucl. Instr. Meth. **A479**, 1 (2002).

[2] B. Aubert *et al.* [BABAR Collaboration], Phys. Rev. Lett. **90**, 242001 (2003).

[3] D. Besson *et al.* [CLEO Collaboration], Phys. Rev. D **68**, 032002 (2003).

[4] B. Aubert *et al.* [BABAR Collaboration], Phys. Rev. D **69**, 031101 (2004).

[5] K. Abe *et al.* [Belle Collaboration], Phys. Rev. Lett. **92**, 012002 (2004).

[6] R. N. Cahn and J. D. Jackson, Phys. Rev. D **68**, 037502 (2003).

[7] W. A. Bardeen, E. J. Eichten and C. T. Hill, Phys. Rev. D **68**, 054024 (2003).

[8] Y. B. Dai, C. S. Huang, C. Liu and S. L. Zhu, Phys. Rev. D **68**, 114011 (2003).

[9] A. Deandrea, G. Nardulli and A. D. Polosa, Phys. Rev. D **68**, 097501 (2003).

[10] T. Barnes, F. E. Close and H. J. Lipkin, Phys. Rev. D **68**, 054006 (2003).

[11] E. van Beveren and G. Rupp, Phys. Rev. Lett. **91**, 012003 (2003).

[12] H. Y. Cheng and W. S. Hou, Phys. Lett. B **566**, 193 (2003).

[13] A. P. Szczepaniak, Phys. Lett. B **567**, 23 (2003).

[14] T. E. Browder, S. Pakvasa and A. A. Petrov, Phys. Lett. B **578**, 365 (2004).

[15] B. Aubert *et al.* [BABAR Collaboration], Phys. Rev. Lett. **93**, 181801 (2004).

[16] B. Aubert *et al.* [BABAR Collaboration], arXiv:hep-ex/0408067.

[17] B. Aubert *et al.* [BABAR Collaboration], arXiv:hep-ex/0406022.

[18] B. Aubert *et al.* [BABAR Collaboration], arXiv:hep-ex/0408087.

[19] S. K. Choi *et al.* [Belle Collaboration], Phys. Rev. Lett. **91**, 262001 (2003).

[20] D. Acosta *et al.* [CDF II Collaboration], Phys. Rev. Lett. **93**, 072001 (2004).

[21] E. J. Eichten, K. Lane and C. Quigg, Phys. Rev. Lett. **89**, 162002 (2002); E. J. Eichten, K. Lane and C. Quigg, Phys. Rev. D **69**, 094019 (2004).

[22] S. Pakvasa and M. Suzuki, Phys. Lett. B **579**, 67 (2004); N. A. Tornqvist, arXiv:hep-ph/0308277; F. E. Close and P. R. Page, Phys. Lett. B **578**, 119 (2004); E. S. Swanson, Phys. Lett. B **588**, 189 (2004); T. Barnes and S. Godfrey, Phys. Rev. D **69**, 054008 (2004); M. B. Voloshin, Phys. Lett. B **579**, 316 (2004).

[23] A. V. Evdokimov *et al.* [SELEX Collaboration], Phys. Rev. Lett. **93**, 242001 (2004).

[24] T. Nakano *et al.* [LEPS Collaboration], Phys. Rev. Lett. **91**, 012002 (2003).

[25] J. Barth *et al.* [SAPHIR Collaboration], Phys. Lett. B **572**, 127 (2003).

[26] V. Kubarovsky *et al.* [CLAS Collaboration], Phys. Rev. Lett. **92**, 032001 (2004).

[27] V. V. Barmin *et al.* [DIANA Collaboration], Phys. Atom. Nucl. **66**, 1715 (2003)

[28] A. Aleev *et al.* [SVD Collaboration], arXiv:hep-ex/0401024.

[29] A. Airapetian *et al.* [HERMES Collaboration], Phys. Lett. B **585**, 213 (2004).

[30] M. Abdel-Bary *et al.* [COSY-TOF Collaboration], Phys. Lett. B **595**, 127 (2004).

[31] C. Alt *et al.* [NA49 Collaboration], Phys. Rev. Lett. **92**, 042003 (2004).

[32] A. Aktas *et al.* [H1 Collaboration], Phys. Lett. B **588**, 17 (2004).

[33] D. Diakonov, V. Petrov and M. V. Polyakov, Z. Phys. A **359**, 305 (1997).

[34] M. Karliner and H. J. Lipkin, Phys. Lett. B **575**, 249 (2003).

[35] R. L. Jaffe and F. Wilczek, Phys. Rev. Lett. **91**, 232003 (2003).

[36] K. Hagiwara *et al.* [Particle Data Group], Phys. Rev. D **66**, 010001 (2002).

[37] B. Wu and B. Q. Ma, Phys. Rev. D **69**, 077501 (2004); H. Walliser and V. B. Kopeliovich, J. Exp. Theor. Phys. **97**, 433 (2003) [Zh. Eksp. Teor. Fiz. **124**, 483 (2003)]; D. Borisyuk, M. Faber and A. Kobushkin, arXiv:hep-ph/0307370.

[38] B. Aubert *et al.* [BABAR Collaboration], arXiv:hep-ex/0408064.

[39] B. Aubert *et al.* [BABAR Collaboration], arXiv:hep-ex/0408037.

[40] T. E. Browder, I. R. Klebanov and D. R. Marlow, Phys. Lett. B **587**, 62 (2004).